Delft University of Technology

Additional Thesis

Effects of a Freshening Boundary Current on Deep Convection and Eddy Activity in the Labrador Sea

by

Tim van Dam

Thesis Committee:

Dr. C. A. Katsman	Environmental Fluid Mechanics	
Dr. S. R. de Roode	Geoscience and Remote Sensing	
S. Georgiou, M.Sc.	Environmental Fluid Mechanics	July 6, 2018

Contents

Chapter 1

Introduction

Global and seasonal variability of the sun's heating of the earth leads to variability in the temperature and salinity of the oceans. Since both temperature and salinity determine the density of the sea water, density differences and hence internal pressure gradients are present throughout the oceans, which drive baroclinic flows (flows driven by density differences). Flows driven by temperature (thermo) and salinity (haline) differences are referred to as thermohaline circulation. The North Atlantic Ocean is the key region for the thermohaline circulation (Pietrzak and Katsman, 2017). As warm saline waters flow towards the North Pole at the surface, they become exposed to extensive surface cooling. The surface waters become colder and hence denser which causes them to sink and subsequently flow back towards the south at depth. This thermohaline circulation on a global scale is sometimes referred to as the great ocean conveyor belt, see Figure 1.1.

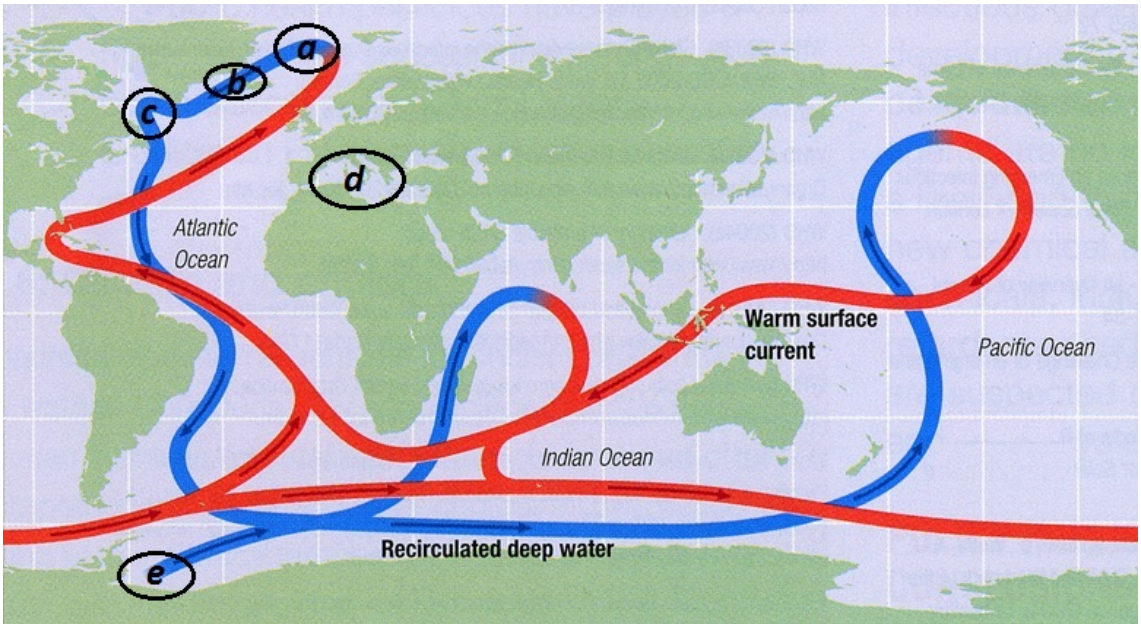

Figure 1.1: Ocean conveyor belt (Modified from *http://www.gurugeografi.id/2017/02/terbentuknya-arus-termohalin.html*) with (a) the Greenland-Iceland-Norwegian (GIN) Seas, (b) the Irminger Sea and (c) the Labrador Sea indicated as the three main deep convection regions of the North Atlantic Ocean. Furthermore, the deep convection regions in the Mediterranean Sea (d) and the Weddell Sea (e) are indicated.

The strength of this circulation is quantified by means of the Atlantic Meridional Overturning Circulation (AMOC), which is the total circulation in meridional direction over the entire width of the basin. The strength of the AMOC shows large variability, both seasonally and interannually. Since the AMOC is responsible for 25 % of the total heat flux from the equator to the poles, it is a crucial and even driving component within the climate system (Pietrzak and Katsman, 2017). Heat carried to higher latitudes by the AMOC is transported to Western Europe by the prevailing Westerlies, which makes the climate milder than in the Eastern USA, right across the Atlantic Ocean. Vice versa, the climate affects the atmospheric conditions and hence the strength of the AMOC (Manabe and Stouffer, 1994). The interchange between climate change and the AMOC, and processes that influence the AMOC is very complex and is something that is not completely understood.

When surface waters become denser than the subsurface layer, the water column becomes statically unstable. The surface waters mix vertically with the lighter subsurface layer until a new stable stratification is reached again. This vertical mixing of water masses is referred to as deep convection (Marshall and Schott, 1999). Deep convection occurs in areas where atmospheric conditions are favorable. Examples of deep convection regions are the North Atlantic Ocean, the Weddell Sea and the Mediterranean Sea, see Figure 1.1. Cyclonic circulation causes divergent mass transport in the gyre at the surface due to Ekman transport, which is 90 degrees to the right in the Northern Hemisphere. This leads to upwelling in the center of the gyre, which is also referred to as Ekman suction, and brings dense subsurface layers closer to the surface. In the North Atlantic Ocean, strong atmospheric cooling during the winter months reduces the Sea Surface Temperature (SST). Furthermore, when sea ice is formed, salt rejection increases the Sea Surface Salinity (SSS) and hence the density even further. A combination of the doming of isopycnals and strong atmospheric cooling forms the perfect conditions for deep convection to occur. If convection occurs in the North Atlantic, it usually does in late winter months February and March. In summer, the surface water becomes warmer again and the melting of land and sea ice causes freshening of the sea surface. The sea surface becomes more buoyant and the ocean restratifies again.

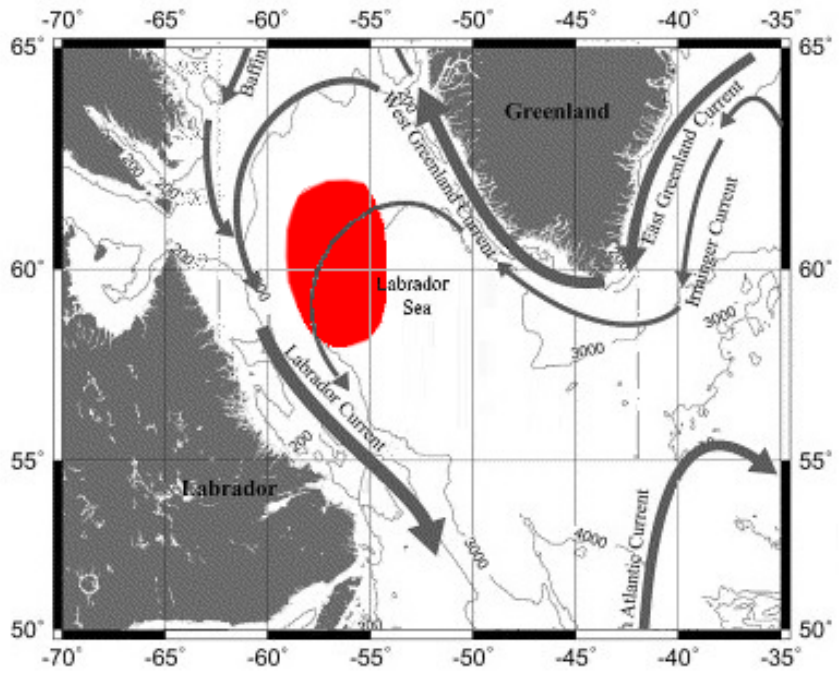

Figure 1.2: Main convection region and currents in the Labrador Sea (from Lilly et al., 2003).

Hypothesis

In the 1970s, the mild winter conditions in combination with freshening of the sea surface, caused the deep convection in the Labrador Sea, see Figure 1.2, to shut down completely for several years (Lilly et al., 1999). The increased fresh water content of the boundary current is also known as a Great Salinity Anomaly (GSA). More and possibly longer lasting anomalies can be expected in the future due to a warming climate and hence the melt of land and sea ice (Ettema et al., 2009). The buoyant water from the boundary current (West Greenland Current and Irminger Current) is carried into the interior of the Labrador Sea by eddies (Prater, 2002). Irminger Rings (IRs), see Figure 2.1, are large eddies that are shed from the Irminger Current off the west coast of Greenland due to the steep topographic slope (Gelderloos et al., 2011) and are efficient in restratifying the Labrador Sea after deep convection (Katsman et al., 2004). The hypothesis is that there are more eddies shed from the boundary current as a consequence of its freshening. From the thermal wind relation, it is known that a horizontal density gradient is balanced by a vertical velocity shear. The increasing salinity difference and hence density difference between the boundary current and the interior is therefore expected to enhance baroclinic instabilities and the shedding of eddies, carrying more and lighter water into the interior of the Labrador Sea. When the sea surface water becomes too light, stratification is preserved, the water column remains statically stable and deep convection does not occur any longer. Since deep convection in the Labrador Sea is of major importance for the strength and variability of the AMOC (Kuhlbrodt et al., 2007), a shutdown of deep Labrador Sea convection may cause the AMOC to shut down, with significant climate change as a consequence (Broecker et al., 1985).

Objective

The main goal of this study is to gain insight in the effect of the freshening of the boundary current (Irminger Current) on deep convection in the Labrador Sea. Since eddy activity plays a major role for the deep convection in the Labrador Sea (Katsman et al., 2004; Chanut et al., 2008), another aim is to quantify how this freshening of the boundary current influences the eddy activity in the interior of the Labrador Sea. In this study it is intended to simulate a shutdown of deep convection by making the surface of the boundary current fresher in order to reproduce the shutdown during the GSA in the 1970s.

Approach

A highly idealized numerical model will be used to perform simulations of different scenarios to quantify the effect of the freshening of the boundary current on deep convection and eddy activity in the interior of the Labrador Sea. To quantify deep convection, the Mixed Layer Depth (MLD) is calculated. The MLD is defined as the depth at which the density is $5 \cdot 10^{-3}$ kg/m^3 higher than the density at the sea surface (Pickart et al., 2002). The eddy activity will be quantified by studying the Eddy Kinetic Energy (EKE). The EKE is defined as the time average of the deviations from the mean flow squared. First the model is introduced in Chapter 2. In Chapter 3, the effect of a freshening boundary current on the MLD is discussed. Chapter 4 discusses the eddy activity and the characteristics of the eddies under different conditions. Chapter 5 combines the results of Chapters 3 and 4 to examine the coherence between eddies, deep convection and the fresh water supply of the boundary current. Finally, Chapter 6 summarizes and discusses the model results of this study.

Chapter 2

Model Setup

Numerical simulations are performed using the MIT general circulation model. Three different scerarios are considered (see Table 2.1): In *Constant35*, which is the reference simulation, the salinity has a constant value of 35 PSU. In *Seas* a seasonal variation of the salinity in the surface layer of the boundary current is implemented in the model as shown in Figure 2.2. Finally, *GSA* represents the scenario where a persistent fresh water anomaly (Great Salinity Anomaly) takes place.

Scenario Name	Description	Salinity	Simulation Time
Constant35	Constant salinity	35 PSU	20 years
Seas	Seasonal salinity variation	34 - 35 PSU	20 years
GSA	Fresh water anomaly after Seas	34 PSU	20 + 5 years

Table 2.1: Characteristics of the different scenarios. The column "Salinity" represents the salinity of the upper layer of the boundary current at the inflow. See text for a more detailed explanation.

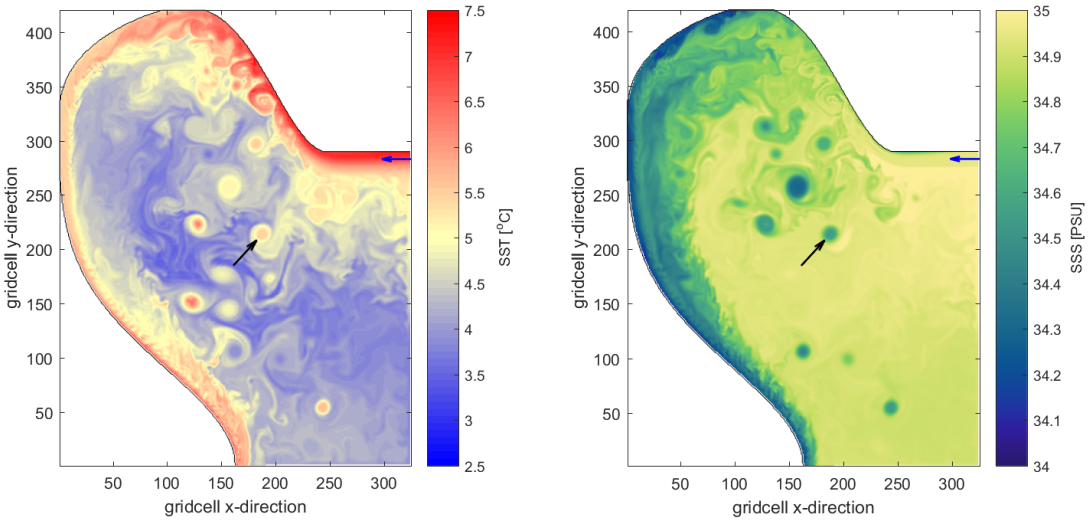

Figure 2.1: Model domain of the Labrador Sea showing a snapshot of the SST (left) and the SSS (right) in December of year 20 in Seas. The black arrow is pointing at an Irminger Ring and the inflow boundary, representing the Irminger Current, is indicated by the blue arrow.

In a recent study (Georgiou et al., 2017), an idealized numerical model of the Labrador Sea is used to investigate the effect of eddies on the deep convection and downwelling in this region. The seasonal variation of the meteorological forcing has been implemented in the model by means of a heat flux Q $[W/m^2]$. Furthermore, the temperature and velocity of the boundary current at the eastern boundary vary throughout the year such that they are in thermal wind balance. Since the study of Georgiou et al. (2017) is mainly focused on the role of eddies, the salinity has been taken constant over the entire domain. The density of the water is therefore calculated with a simplified linear equation of state, only depending on temperature differences: $\rho = \rho_0(1-\alpha(T-T_0))$, with ρ_0 the reference density, α the thermal expansion coefficient, T the temperature and T_0 the reference temperature (5.37 ^{o}C). The model setup of Georgiou et al. (2017) is referred to as the reference run, Constant35.

For the purpose of this study, new boundary conditions have been constructed in order to account for the seasonal salinity variation of the boundary current. In Seas, the SSS at the inflow at the eastern boundary, see Figure 2.1, varies from $34-35$ PSU and reaches its minimum in July and its maximum in January. In order to study the effect of the SSS of the boundary current, the temperature, heat flux and other model forcing is equal to the model forcing in Constant35 (after Georgiou et al., 2017). The monthly varying temperature and salinity in the upper layer of the boundary current at the eastern boundary are shown in Figure 2.2. Since the salinity is no longer constant, the density now also depends on salinity differences. The simplified linear equation of state for the calculation of the density now becomes: $\rho = \rho_0(1 - \alpha(T - T_0) + \beta(S - S_0))$, where β denotes the haline contraction coefficient, S the salinity and S_0 the reference salinity (35 PSU).

To represent the GSA of the 1970s, a scenario is constructed in which the SSS at the inflow at the eastern boundary has a constant value of 34 PSU after year 20 of Seas. SSS observations of the Labrador Sea during the GSA of the 1970s show salinity anomalies of the boundary current off the coast of Greenland in the same order of magnitude (Belkin et al., 1998; Belkin, 2004).

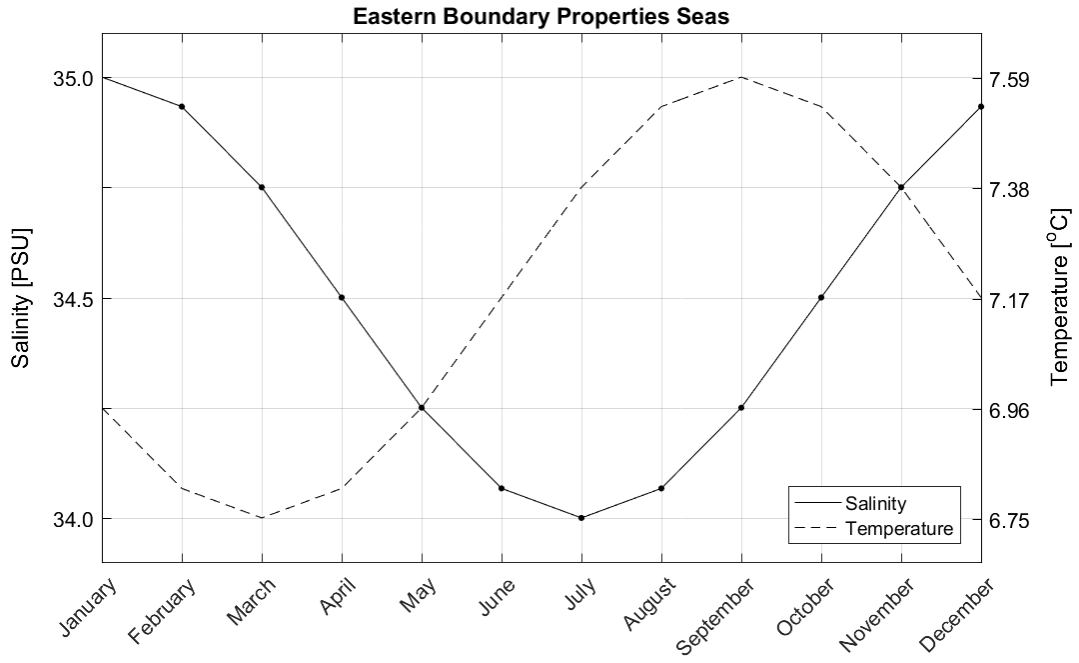

Figure 2.2: The imposed SSS (solid line) and SST (dashed line) of the boundary current at the inflow at the eastern boundary in Seas.

Figure 2.2 shows that there is a phase shift between the minima and maxima of the SSS and SST of the boundary current. The individual contributions of the salinity and temperature differences on the density of the surface of the boundary current are calculated using the equation of state (Figure 2.3). The density difference due to salinity variations is equal to $\Delta\rho_S = \rho_0\ \beta\ (S - S_0)$, with a haline contraction coefficient of $\beta = 7.5 \cdot 10^{-4}$ PSU^{-1}. The density difference due to changes in temperature is equal to $\Delta\rho_T = -\rho_0\ \alpha\ (T - T_0)$, with a thermal expansion coefficient of $\alpha = 1.7 \cdot 10^{-4}$ K^{-1}.

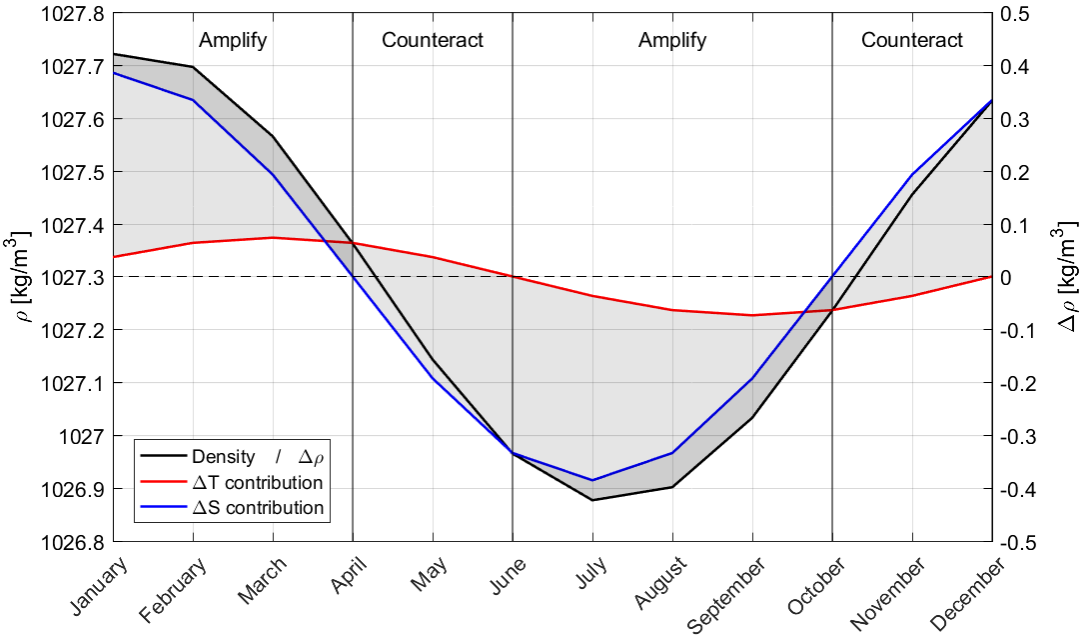

Figure 2.3: Individual contributions of the SSS (blue line) and SST (red line) variations of the boundary current to density differences (black line) can be read from the right axis. From the left axis, the density can be read (black line). The dotted line represents the time average surface density of the boundary current at the inflow. The dark hatched area indicates amplification of salinity and temperature variations.

Figure 2.3 shows that the density of the sea surface of the boundary current is dominated by the variations in salinity. However, due to the shift of the temperature variation, the density has a small phase lag with respect to the salinity. In the months January to April, the high salinity and low temperature amplify each other to form dense surface water of the boundary current. From April to June, their contributions counteract since the still low temperature makes the water more dense, but the decrease in salinity makes the water more buoyant. From June to October, the low salinity and high temperature of the boundary current amplify each other again to form light water. From October to December they counteract again due to the increasing salinity and the still relatively warm surface water.

Chapter 3

Analysis of the MLD

In this chapter the deep convection in the Labrador Sea is analyzed by studying the MLD. The MLD can be seen as the thickness of the statically unstable water colum over which vertical mixing of water mass takes place. The MLD is defined as the depth at which the density is $5 \cdot 10^{-3}\ kg/m^3$ higher than the density at the surface (Pickart et al., 2002). For each scenario, the mean winter (February and March) MLD over the last five years of simulation is shown in Figure 3.1. Note that the time frame of GSA is different from constant35 and Seas (See Table 2.1): the considered years for the analysis are years 16 - 20 for Constant35 and Seas and years 21 - 25 for GSA.

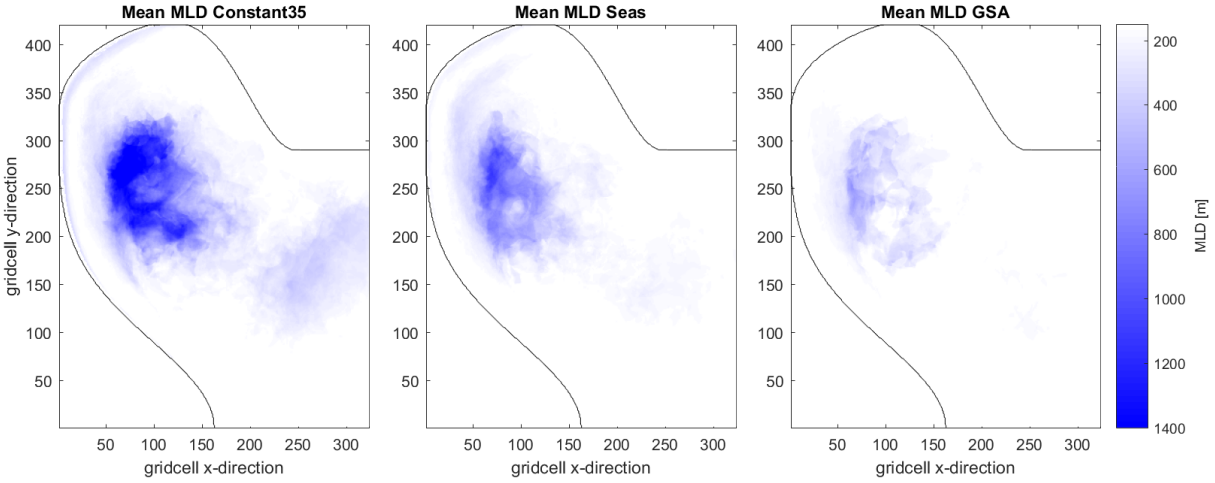

Figure 3.1: The mean winter (Februari and March) MLD of the last five years of Constant35 (a), Seas (b) and GSA (c).

Figures 3.1a to 3.1c show that the salinity has a significant effect on the MLD. The five year averaged winter MLD reaches only 1150 meters in Seas (Figure 3.1b) where the maximum of the five year average in Constant35 is almost 1800 meters (Figure 3.1a). The mean winter MLD in GSA is again much shallower, the five year average only reaches 700 meter (Figure 3.1c). However, throughout the five years from which the latter average is calculated, the system is still adapting towards a new equilibrium (see Figure 3.2b). Therefore it is informative to look at the development of the MLD over time.

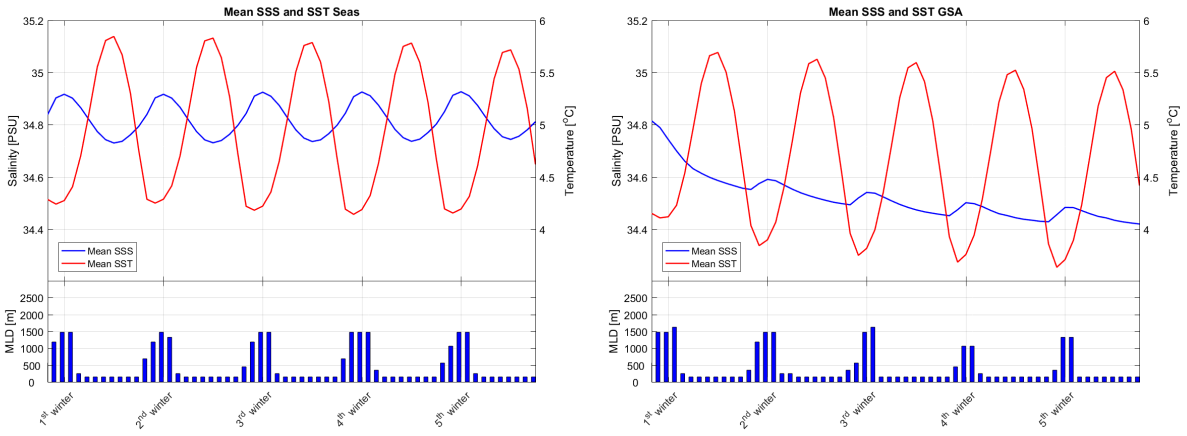

(a) (b)

Figure 3.2: Mean SSS (blue line), SST (red line) and maximum MLD (blue bars) during the last five years of simulation of Seas (a) and GSA (b).

Figure 3.2 shows that the system has reached an equilibrium in Seas (Figure 3.2a), but that GSA is still adapting (Figure 3.2b). Figure 3.2b clearly shows that the freshening of the sea surface, due to the fresh water anomaly, is causing a decay of the MLD. It also illustrates that there is an interplay between the maximum MLD and the mean SSS: The sea surface becomes fresher until deep convection occurs in the late winter months. Vertical mixing brings saltier water from depth to the surface and increases the SSS, even in GSA, where there is a constant fresh water supply.

In Figure 3.3, on the left, an area, "*Area1*" is indicated where the strongest deep convection occurs. The MLD inside Area1 is mapped to a horizontal section, "*MaxMLDx*", by taking the maximum value over the meridional direction at each gridcell in x-direction. The right figure shows the interannual variability of the mean MLD inside Area1 for all three scenarios. The time is denoted by the number of years within the last five years of each simulation.

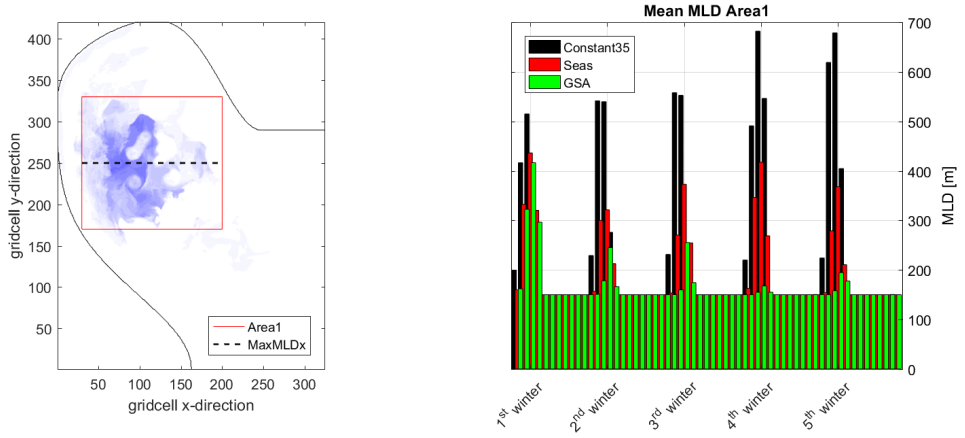

Figure 3.3: Left: the MLD inside a deep convection area (Area1, red box) is mapped to a longitudonal section (MaxMLDx, black dashed line) by taking the maximum over the meridional direction. Right: the mean MLD inside Area1 as a function of time in Constant35 (black), Seas (red) and GSA (green).

Figure 3.3 illustrates that the MLD is strongly influenced by the salinity of the boundary current. In Constant35 the mean MLD is approximately 500 - 600 meters, while it is only 300 - 400 meters in Seas. In GSA, there is a clear decreasing trend of the mean MLD, since it is not in equilibrium. In the first year of the salinity anomaly, the mean MLD is 300 - 400 meters but three years later it has almost disappeared. This seems, however, contradictory to Figure 3.2b, which shows that there is still deep convection reaching a depth of almost 1400 meters. This suggests that size of the deep convection area is strongly influenced by the fresh water supply of the boundary current.

Figures 3.4a - 3.4c show the interannual variability of MaxMLDx, as defined in Figure 3.3.

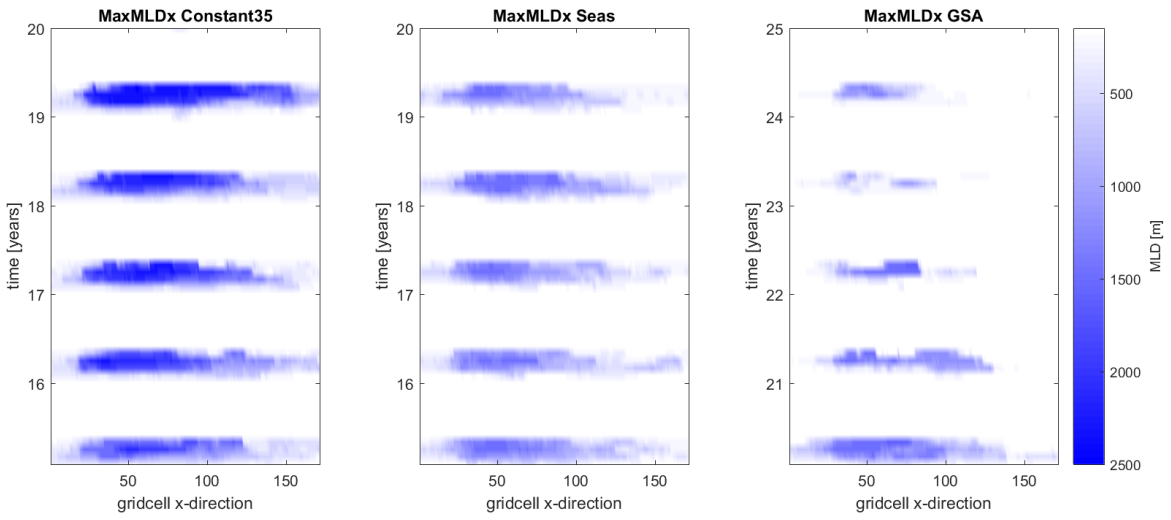

(a) (b) (c)

Figure 3.4: MaxMLDx, as described in Figure 3.3, as a function of time (vertical axis) for Constant35 (a), Seas (b) and GSA (c).

Figure 3.4 illustrates that the magnitude of the MLD is strongly affected by the SSS of the boundary current. In constant35 (Figure 3.4a), the maximum MLD is in the order of 2500 meters every year, while the maximum MLD in Seas (Figure 3.4b) and GSA (Figure 3.4c) is in the order of 1500 meters. It is notable that the fresh water anomaly introduced in GSA strongly affects the size of the convection area, and therefore the amount of convection, but does not lead to a shutdown. Despite the fresh water anomaly, there is still deep convection after five years.

Figure 3.4 also shows that the location and magnitude of the MLD show (some) interannual variability in all scenarios. More specifically, there is an interannual variability in how far the deep convection area extends towards the eastern part of the Labrador Sea. Especially in GSA (Figure 3.4c), the deep convection in the eastern part of the Labrador Sea is strongly suppressed, due to the low SSS of the boundary current. Since the eastern part of the region is near the coast of Greenland, where IRs are shed from the boundary current, it is expected that eddies play an important role in the occurence of deep convection.

Chapter 4

Eddy Activity

In this chapter, the effect of fresh water on the eddy activity in (the interior of) the Labrador Sea is analyzed. According to the thermal wind balance, a density gradient in horizontal direction is balanced by a velocity shear in the vertical direction:

$$\rho_0 f \frac{\partial v}{\partial z} = -g \frac{\partial \rho}{\partial x}, \qquad \rho_0 f \frac{\partial u}{\partial z} = g \frac{\partial \rho}{\partial y}$$

Since a fresher boundary current leads to a larger density gradient in the horizontal direction, it is expected that this is associated with more baroclinic instabilities and shedding of eddies. Figures 4.1a to 4.1c show snapshots of the absolute velocity for the three scenarios.

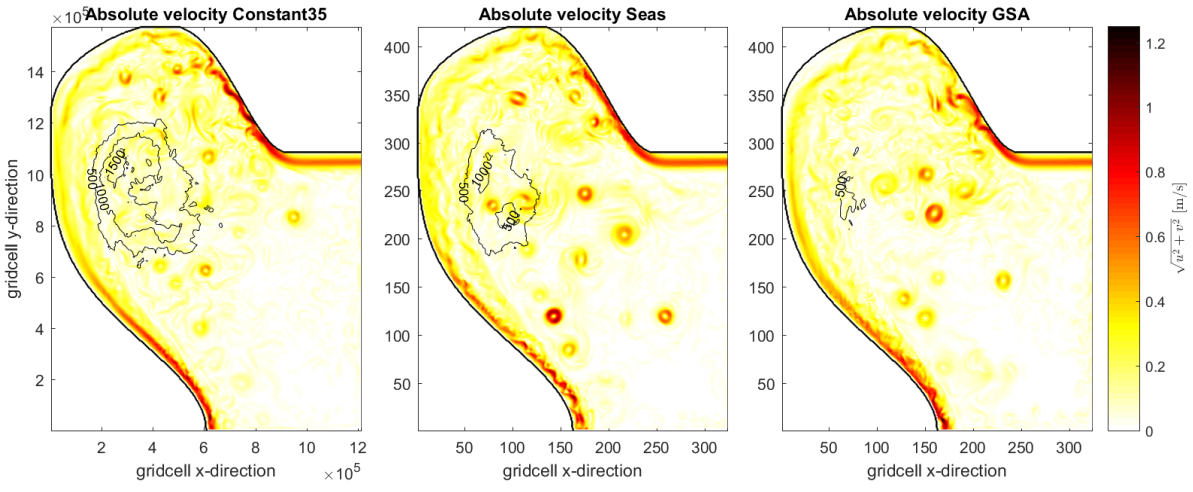

(a) (b) (c)

Figure 4.1: Snapshot of the absolute velocity in the last July of Constant35 (a), Seas (b) and GSA (c). The black lines indicate the 500 meter contours of the mean MLD (as plotted in Figure 3.1).

Figure 4.1 shows that the fresher boundary current ($S = 34$ PSU in July) in Seas (Figure 4.1b) and in GSA (Figure 4.1c) leads to stronger and larger eddies in the interior of the Labrador Sea, compared

to Constant35 (Figure 4.1a), see also the next section and Figure 4.4. The "strength" of the eddies is not only a measure of their velocity shear and size, but is also quantified by the density shear in the horizontal direction. The effect of the lower SSS of the boundary current on the eddy activity is quantified by analyzing the EKE in the next section.

Eddy Kinetic Energy

Using the Reynolds decomposition, a velocity can be expressed in a mean flow and a deviation from this mean motion: $u = \overline{u} + u'$, where $\overline{u}$ denotes the time average flow and u' the deviation from this time average flow. The EKE is defined as the time averaged (denoted by the overbar) square of the deviations (u' and v'):

$$EKE = \frac{1}{2}(\overline{u'^2 + v'^2})$$

In this study, the time average velocities $\overline{u}$ and $\overline{v}$ as well as the EKE are calculated over the last five years of simulation. First $\overline{u}$ and $\overline{v}$ are calculated from the monthly mean velocities at the surface. Subsequently, the deviations u' and v' are calculated from the snapshots. Figure 4.2 shows the five year average EKE of the last five years of each simulation.

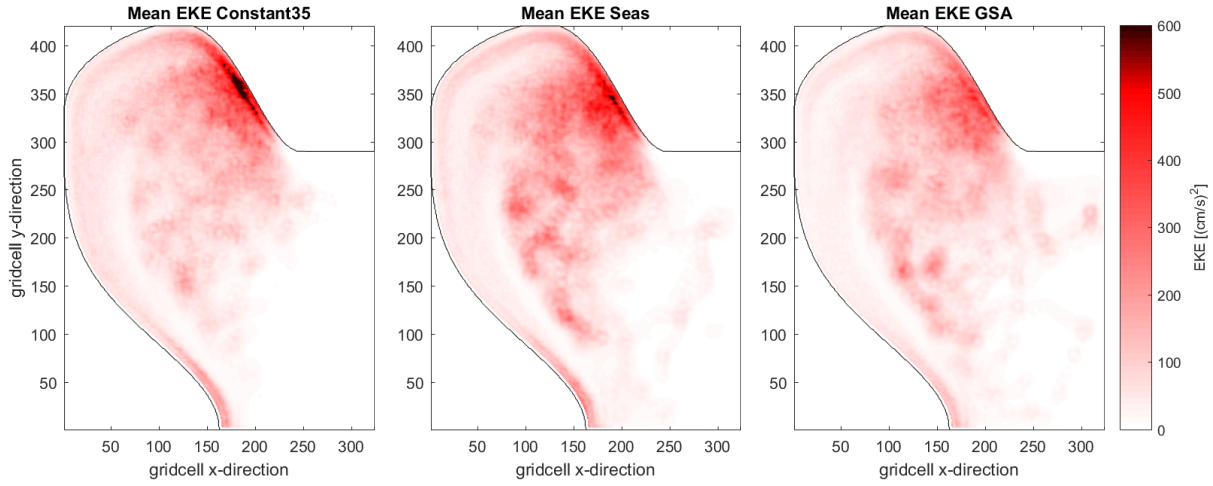

(a) (b) (c)

Figure 4.2: The five year average EKE [$(cm/s)^2$] in Constant35 (a), Seas (b) and GSA (c).

The eddy activity near the boundary current, where the eddies are shed, is higher in Constant35 than in Seas (Figure 4.2b) and GSA (Figure 4.2c). In Seas (Figure 4.2a), five year average values of the EKE exceed 700 $(cm/s)^2$ near the coast of Greenland while it only reaches 630 $(cm/s)^2$ in Seas (Figure 4.3b) and 450 $(cm/s)^2$ in GSA (Figure 4.3c). A possible explanation is that the low SSS of the boundary current increases the baroclinic instability and cause IRs to shed earlier from the boundary current in Seas and GSA than in Constant35, where it remains more stable.

In the interior of the Labrador Sea however, the EKE is higher in Seas and GSA, compared to Constant35. The mean interior EKE (averaged over the last five years and the whole interior of the Labrador Sea) amounts to 105 $(cm/s)^2$ in Seas, 75 $(cm/s)^2$ in GSA and 73 $(cm/s)^2$ in Constant35.

The EKE in the interior of the Labrador Sea is higher in Seas and GSA because the eddies carrying fresh water live longer and travel further into the domain (see also Figures 4.3 and 4.4).Furthermore, the fresher boundary current possibly enhances instability of the boundary current which leads to more intense shedding of IRs.

Note that here the interior is defined as Area1, with exclusion of the boundary current, and is therefore limited to the deep convection area only. The high EKE south of this area is not included in this representation of the mean. Furthermore, GSA is not in equilibrium (see Figure 3.3).

The EKE inside Area1 is mapped to a longitudinal section "*MaxEKEx*" by taking the maximum value of the EKE in y-direction at every x-gridcell (just like for MaxMLDx, Figure 3.3). Figure 4.3 shows the seasonal and interannual variability of MaxEKEx during the last five years of each simulation. For better visibility and a more meaningful interpretation of the results, values of the EKE < 1200 $(\mathrm{cm/s})^2$ are omitted in the figure below.

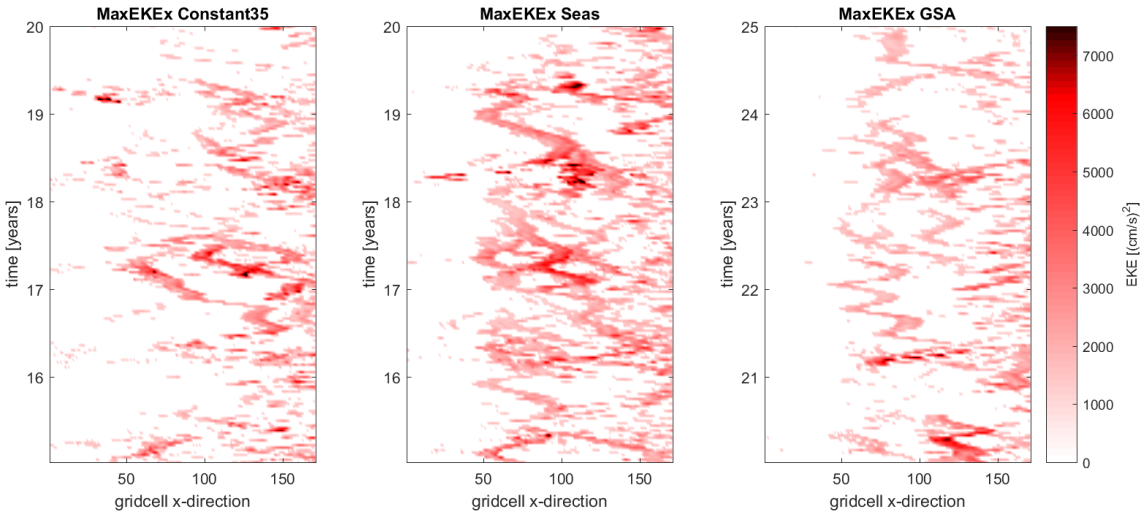

Figure 4.3: MaxEKEx as a function of time (vertical axis) for Constant35 (a), Seas (b) and GSA (c).

Figure 4.3 illustrates that high values of the EKE in the western - central part of Area1 (e.g. x-gridcells 50 - 100) are more persistent and prominent in Seas (Figure 4.3b) and GSA (Figure 4.3c) than in constant35 (Figure 4.3a). Furthermore, certain paths of eddies can be identified which reveals that the eddies in Seas and GSA live longer (longer than one year) than the eddies in Constant35 (up to a year). The hypothesis is that this can be contributed to the salinity of the boundary current; The velocity shear of the eddies in Constant35 is in balance with a strictly temperature related density gradient. The eddies in Seas and GSA carry fresh water, which also contributes to the density gradient. The eddies shed from the boundary current travel further into the interior and preserve their energy longer when they carry fresh water.

To verify wether this statement is justified or not, an eddy is traced from the moment it is shed from the boundary current, near the coast of West Greenland, in the last January of each simulation. A longitudinal cross section of an eddy for each scenario is shown in Figure 4.4 by means of three snapshots, three months apart.

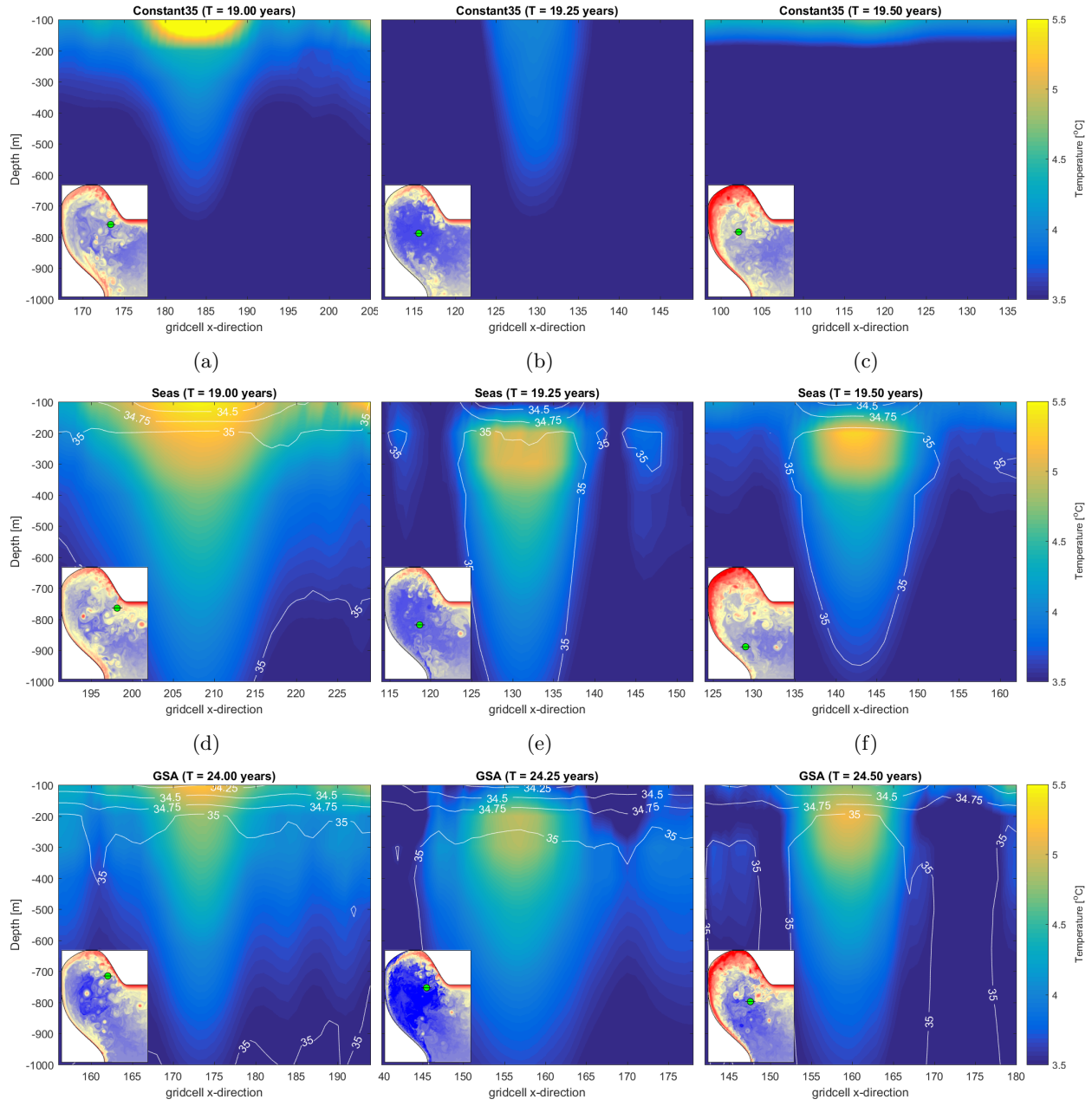

Figure 4.4: Cross section of an eddy that is shed from the boundary current. The colors indicate the temperature and the white contours show the salinity. The maps in the bottom left show the SST and the position of the eddy (green dot). The top three figures show an eddy in Constant35 in January (4.4a), April (4.4b) and July (4.4c). The middle three figures (4.4d - 4.4f) show an eddy in Seas and the bottom three (4.4g - 4.4i) show an eddy in GSA in the same months.

Figure 4.4 illustrates that an eddy carrying fresh water preserves its density gradient with respect to the ambient water and hence its energy much longer. After half a year, the eddy in Constant 35

is almost completely dissipated (Figure 4.4c), but in Seas (Figure 4.4f) and GSA (Figure 4.4i) their structure is still clearly visible. In the latter two simulations, a clear "fresh cap" can be distinguished at the surface, which is preserved until the end of the simulations. The vertical structure of the eddies agrees very well with observations (Hatun et al., 2007) and (other) eddy-resolving model studies (Kawasaki and Hasumi, 2004); The eddies (IRs) contain fresh, cold water at the surface and a warm saline core at depth. As stated earlier, based on the analysis of the absolute horizontal velocities (Figure 4.1), the eddies carrying fresh water appear to be stronger, regarding the orbital velocity. Furthermore, the density gradient between the eddies and the ambient water is significantly larger when the core of the eddy contains fresh water at the surface and haline water at depth.

The eddy in Constant35 is maintained by a temperature gradient, which is dissipated quickly as the eddy enters the interior of the Labrador Sea and is exposed to severe cooling at the surface. The eddy in Seas is also cooled as it enters the interior (note the fresh, cold cap in Figures 4.4e and 4.4f). Its "freshness" is however retained due to the absence of a salinity flux at the surface. This ensures the preservation of a density gradient and hence velocity shear and allow the eddies in Seas and GSA to wander through the interior of the Labrador Sea much longer than in Constant35.

Figure 4.4 also shows that the eddies carrying fresh water are larger in both horizontal (diameter) and vertical extent. This could already be observed from Figure 4.1. A typical maximum eddy diameter in the interior of the Labrador Sea is in the order of 60 km in Constant35. In Seas and GSA, larger eddies with a diameter in the order of 80 km are typically found, see Figure 4.5.

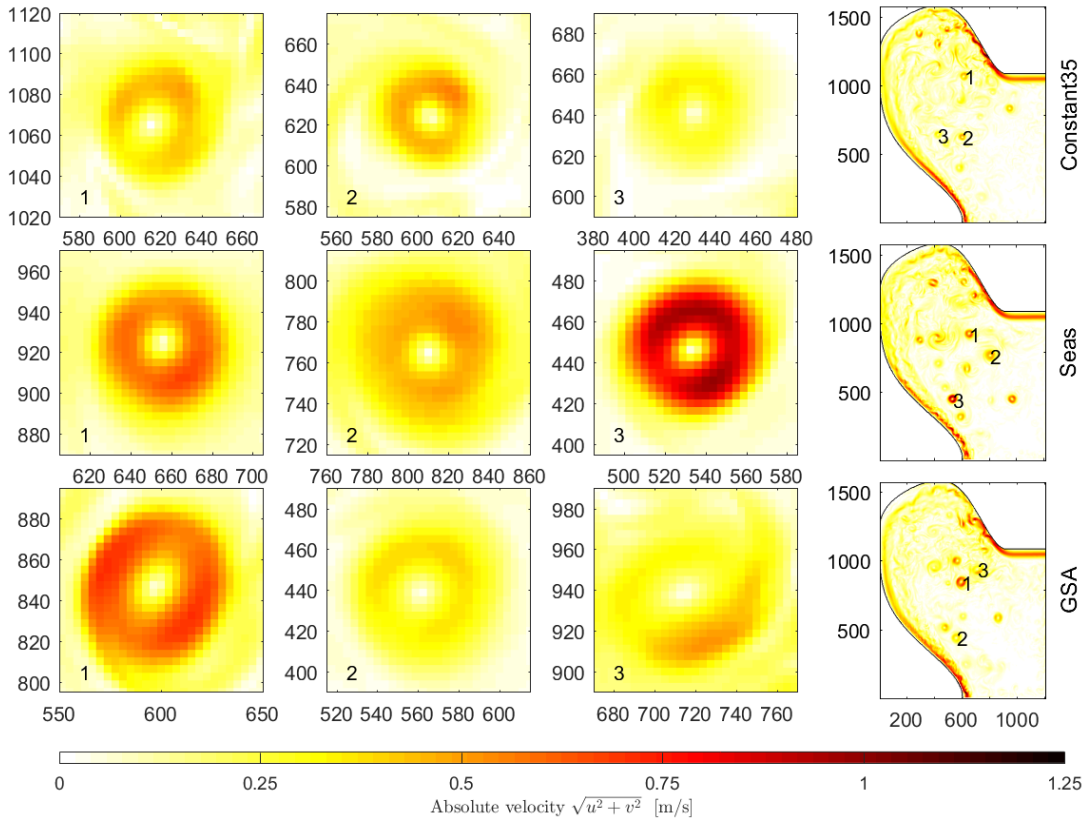

Figure 4.5: Absolute velocity at the sea surface in the last July of each simulation. The left three columns show three typical eddies in Constant35 (top), Seas (middle) and GSA (bottom). The figures in the most right column show the locations of the eddies.

Chapter 5

Interplay between Eddies and Deep Convection

Chapters 3 and 4 show that both the MLD and EKE have a large spatial, seasonal and interannual variability. In this chapter the model results of the analysis of the MLD (Chapter 3) and the eddy activity (Chapter 4) are examined simultaneously to study the coherence of the eddy activity, deep convection and the properties of the boundary current.

In Figure 5.1, the EKE, MLD and the density at the sea surface are plotted together. The EKE is averaged over the last five years of each simulation. The MLD, however, is only present during deep convection. Therefore the MLD and sea surface density are averaged over only the winter months (February and March) of the last five years of the each simulation.

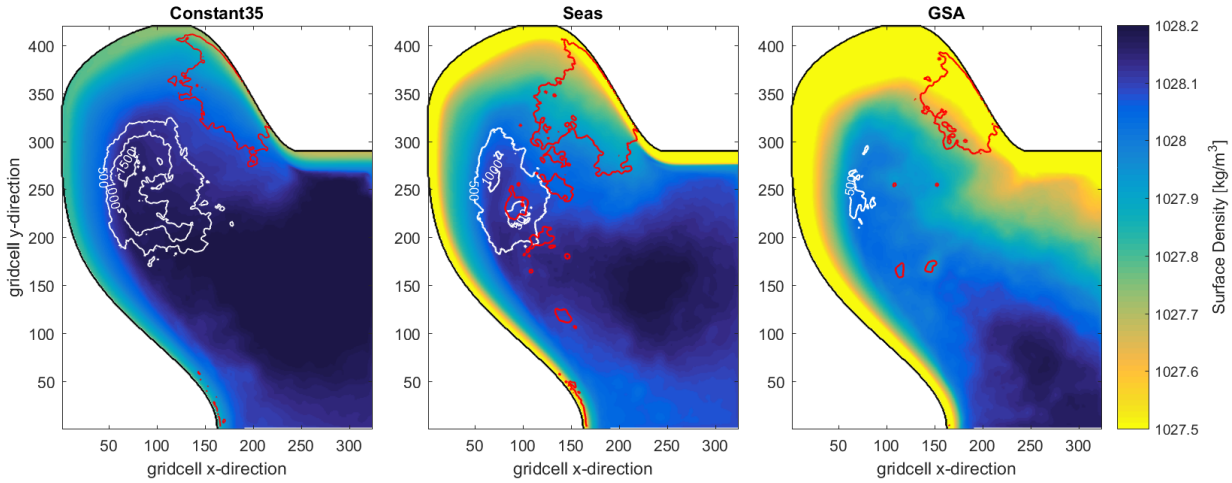

(a) (b) (c)

Figure 5.1: The five year average winter (Feb - March) sea surface density (colors) of the Labrador Sea in Constant35 (a), Seas (b) and GSA (c). The white contours indicate the five year average winter MLD and the 200 $(cm/s)^2$ contour of the five year mean EKE is shown in red.

Figure 5.1 reveals a relation between the lateral spreading of the EKE and the lateral extent of the deep convection region. In Constant35 (Figure 5.1a) the high EKE is concentrated near the boundary current and the MLD (reaching 1800 meters) extents to the central part of the Labrador Sea. In Seas (Figure 5.1b) the high EKE is more spread towards the central and even the south-western part of the Labrador Sea. The MLD is much shallower (reaching 1150 meters) and is more restricted to the Western Labrador Sea. Furthermore, the sea surface density follows the EKE contour due to the buoyant water that is transported by the eddies. IRs bring buoyant water from the boundary current to the interior and confine the deep convection to the Western Labrador Sea. In GSA (Figure 5.1c), the lateral spreading of high EKE is limited to the boundary current and the MLD is confined to the far Western Labrador Sea, reaching only 700 meters. The constant supply of fresh water of the boundary current causes a pursuing freshening of the sea surface (see Figure 3.2b) and hence enhances stratification (see also Figure 4.4g - 4.4i).

To study the seasonal and interannual interaction between the eddy activity and the deep convection, the EKE and MLD inside Area1 are compared in Figure 5.2. Because high EKE suppresses deep convection, the values of MaxMLDx and MaxEKEx are most likely obtained from different latitudes, which makes the "simultaneous" analysis meaningless. Therefore, at every gridcell in x-direction, the mean value of all cells in y-direction (instead of the maximum, like MaxMLDx and MaxEKEx) is mapped to a horizontal section; "MeanMLDx" represents the MLD and "MeanEKEx" represents the EKE inside Area1. For better visibility, low values of MeanEKEx (< 200 $(\mathrm{cm/s})^2$) are omitted.

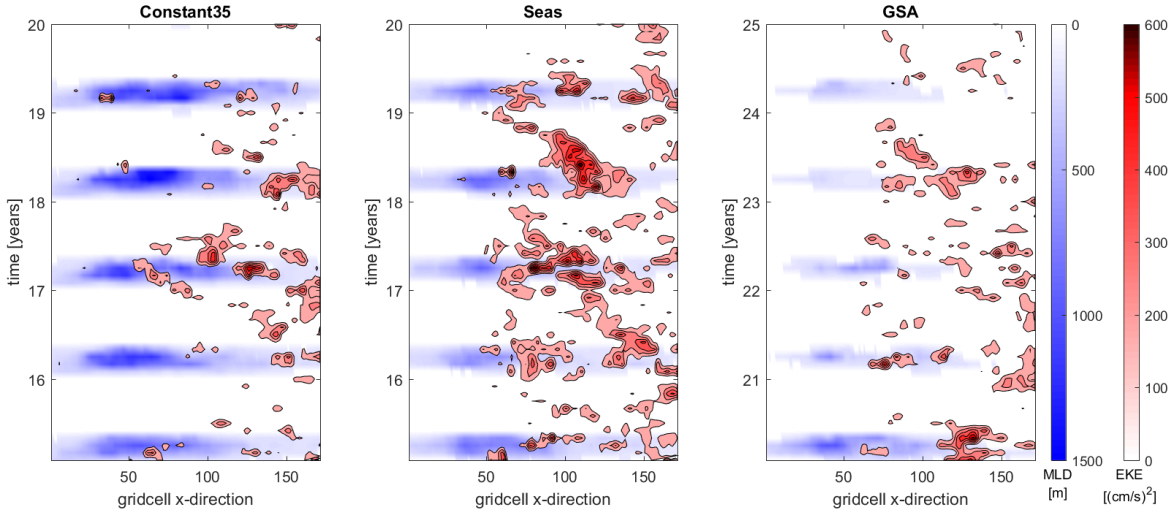

(a) (b) (c)

Figure 5.2: MeanMLDx (blue shading) and MeanEKEx (Red contours) as a function of time (vertical axis) for Constant35 (a), Seas (b) and GSA (c).

Figure 5.2 shows that the mean EKE contours confine the deep convection to the West. Not only do the eddies play a role in the restratification of the Labrador Sea, they also inhibit deep convection.

Chapter 6

Summary and Discussion

This chapter summarizes and discusses the model results of the preceding chapters.

Summary

The large impact on and interchange with the climate necessitates a better understanding of the processes and phenomena that drive or influence deep convection. This study addresses the role of the freshening of the boundary current (Irminger Current and West Greenland Current) on the deep convection, the eddy activity and the interplay between them in the Labrador Sea. Using an idealized numerical model of the Labrador Sea, three scenarios, Constant35 ($S = 35$ PSU), Seas ($S = 34 - 35$ PSU) and GSA ($S = 34$ PSU), see Table 2.1, are simulated to assess the influence of the freshening of the boundary current on deep convection and, more specifically, its contribution to the shutdown of the AMOC in the 1970s.

The analysis of the MLD in Chapter 3 reveals that a freshening of the boundary current suppresses deep convection. The five year average winter MLD reaches 1800 meters in Constant35, 1150 meters in Seas and only 700 meters in GSA. Furthermore, the size of the deep convection region, and its horizontal extent towards the east in particular, is strongly affected by the salinity of the boundary current (see Figures 3.1 and 3.4). In constant35 the deep convection region extends up to 800 km from the western boundary of the model domain. In Seas the deep convection region is more limited to the western and central part of the Labrador Sea (650 km) and in GSA deep convection is limited further to the West Labrador Sea (up to 450 km in the last years of simulation), see Figure 3.4.

Chapter 4 shows that the EKE is more concentrated near the boundary current in Constant35 than in Seas, and GSA, where the EKE is laterally spread more towards the Western Labrador Sea. In Seas, the EKE is significantly higher in the interior (105 $(\mathrm{cm/s})^2$, interior averaged) than in Constant35 (73 $(\mathrm{cm/s})^2$) and GSA (75 $(\mathrm{cm/s})^2$). In GSA, however, the EKE decreases in time as the anomaly persists. The IRs in Constant35 are smaller in vertical and lateral extent and are dissipated quicker because their density gradient with respect to the ambient water is strictly temperature related. In Seas and GSA the eddies are larger and transport fresh water, which conserves the density gradient much longer. This allows them to travel further into the domain and transport more buoyancy into the interior. In GSA the EKE decreases in time as the salinity anomaly persists.

Chapter 5 indicates a strong coherence between the salinity of the boundary current, eddy activity and deep convection. In Constant35, the eddies are dissipated fairly quickly by the surface cooling as they travel into the interior, which "allows" for deep convection to a large extent. In Seas, the eddies

retain their freshness and travel further into the domain, bringing more buoyant water to the interior and confining deep convection more towards the Western Labrador Sea (which was also suggested by Pickart et al., 2002). In GSA, however, the coherence between the EKE and the MLD is less evident. Figure 5.2c suggests that the EKE confines the very shallow deep convection (500 m) towards the west, but EKE values are relatively low (200 - 300 $(cm/s)^2$). Therefore the suppression of deep convection must be dominated by the sea surface density, which is significantly lower due to the constant supply of fresh water.

Discussion

This study shows that a salinity anomaly affects the shedding, strength and life time of eddies significantly. Due to the increased buoyancy transport and eddy activity in the interior of the Labrador Sea, deep convection is inhibited and more specifically, confined further towards the Western Labrador Sea. This study also shows that a (long lasting) salinity anomaly increases the SSS and reduces the EKE in the interior of the Labrador Sea on the long term. It can be stated that a GSA inhibits deep convection but is not sufficient to lead to a complete shutdown. This indicates the importance of the mild winter conditions for the shutdown of the 1970s.

Due to the persisting anomaly, the sea surface (and also subsurface) of the interior of the Labrador becomes fresher in time (see Figure 3.2b). This is believed to reduce the density gradient between the boundary current and the interior of the Labrador Sea and hence the shedding of IRs. Bracco et al. (2008) argued that the variability in the structure of the boundary current could be responsible for the interannual variability in the shedding of IRs. De Jong et al. (2016) also showed a strong correlation between the time variability of the EKE and the density difference between the boundary current and the interior. Further investigation needs to be carried out to asses the actual effect of a salinity anomaly of the boundary current on the formation of IRs.

With the current model forcing and boundary conditions, the model was not able to reproduce a shutdown of deep convection. Even in GSA when the anomaly persists for 20 years, although it is very weak, there are still signs of deep convection. As was mentioned earlier, the mild winter conditions of the 1970s, and thus a lack of atmospheric cooling, contributed to the shutdown of deep convection in the Labrador Sea. Lilly et al. (1999) argued that the weak atmospheric cooling was primarily responsible for the 1970s shutdown of deep convection rather than the salinity anomaly. In this study however, the surface cooling does not vary interannually and is equal to the surface cooling in Seas (after Georgiou et al., 2017). In order to mimic the mild winter conditions of the 1970s, new heat fluxes have to be designed.

Furthermore, there is no salinity flux imposed at the surface, which might lead to over-estimation of the preservation of an eddies' density gradient. Hence, the life time of the eddies in Seas and GSA might be unrealistically long. For a more correct incorporation of salinity variations, a fresh water (precipitation) and/or salt (evaporation) flux should be imposed at the sea surface.

Bibliography

Belkin, I. M. (2004). Propagation of the Great Salinity Anomaly of the 1990s around the northern North Atlantic. *Geophysical Research Letters*, 31(8):L08306.

Belkin, I. M., Levitus, S., Antonov, J., and Malmberg, S. (1998). Great Salinity Anomalies in the North Atlantic. *Progress in Oceanography*, 41:1–68.

Bracco, A., Pedlosky, J., and Pickart, R. S. (2008). Eddy Formation near the West Coast of Greenland. *Journal of Physical Oceanography*, 38:1992–2002.

Broecker, W. S., Peteet, D. M., and Rind, D. (1985). Does the ocean-atmosphere system have more than one stable mode of operation? *Nature*, 315:21–26.

Chanut, J., Barnier, B., Large, W., Debreau, L., Penduff, T., Molines, J. M., and Mathiot, P. (2008). Mesoscale Eddies in the Labrador Sea and Their Contribution to Convection and Restratification. *Journal of Physical Oceanography*, 38:1617–1643.

De Jong, M. F., Bower, A. S., and Furey, H. H. (2016). Seasonal and Interannual Variations of Irminger Ring Formation and Boundary-Interior Heat Exchange in FLAME. *Journal of Physical Oceanography*, 46:1717–1734.

Ettema, J., van den Broeke, M. R., Erik van Meijgaard, E., van de Berg, W. J., Bamber, J. L., Box, J. E., and Bales, R. C. (2009). Higher surface mass balance of the Greenland ice sheet revealed by high-resolution climate modeling. *Geophysical Research Letters*, 36(L12501).

Gelderloos, R., Katsman, C. A., and Drijfhout, S. S. (2011). Assessing the Roles of Three Eddy Types in Restratifying the Labrador Sea after Deep Convection. *Journal of Physical Oceanography*, 41:2102–2119.

Georgiou, S., van den Boog, C. G., Brüggemann, N., Pietrzak, J. D., and Katsman, C. A. (2017). On the interplay between eddies, deep convection and downwelling in the Labrador Sea. 2017.

Hatun, H., Eriksen, C. C., and Rhines, P. B. (2007). Buoyant Eddies Entering the Labrador Sea Observed with Gliders and Altimetry. *Journal of Physical Oceanography*, 37:2838–2854.

Katsman, C. A., Spall, M. A., and Pickart, R. S. (2004). Boundary current eddies and their role in the restratification of the Labrador Sea. *American Meteorological Society*, 34:1967–1983.

Kawasaki, T. and Hasumi, H. (2004). Effect of freshwater from the West Greenland Current on the winter deep convection in the Labrador Sea. *Ocean Modelling*, 75:51–64.

Kuhlbrodt, T., Griesel, A., Montoya, M., Levermann, A., Hofmann, M., and S, R. (2007). On the driving processes of the Atlantic Meridional Overturning Circulation. *Reviews of Geophysics*, 45(RG2001).

Lilly, J. M., Rhines, P. B., Schott, F., Lavender, K., Lazier, J., Send, U., and D'Asaro, E. (2003). Observations of the Labrador Sea eddy field. *Progress in Oceanography*, 59:75–176.

Lilly, J. M., Rhines, P. B., Visbeck, M., Davis, R., Lazier, J. R. N., Schott, F., and Farmer, D. (1999). Observing Deep Convection in the Labrador Sea during Winter 1994/95. *Journal of Physical Oceanography*, 29:2065–2098.

Manabe, S. and Stouffer, R. J. (1994). Multiple-Century Response of a Coupled Ocean-Atmosphere Model to an Increase of Atmospheric Carbon Dioxide. *Journal of Climate*, 7:5–23.

Marshall, J. and Schott, F. (1999). Open-ocean convection: Observations, theory, and models. *Reviews of Geophysics*, 37:1–64.

Pickart, R. S., Torres, D. J., and Clarke, R. A. (2002). Hydrography of the Labrador Sea during Active Convection. *Journal of Physical Oceanography*, 32:428–457.

Pietrzak, J. and Katsman, C. A. (2017). *An Introduction to Oceanography for Civil and Offshore Engineers, Lecture Notes*. Delft University of Technology.

Prater, M. D. (2002). Eddies in the Labrador Sea as Observed by Profiling RAFOS Floats and Remote Sensing. *Journal of Physical Oceanography*, 32:411–427.